

de Sitter Gauge Theory of Gravity: An Alternative Torsion Cosmology

Xi-chen Ao and Xin-zhou Li*

*Shanghai United Center of Astrophysics (SUCA),
Shanghai Normal University, 100 Guilin Road, Shanghai 200234, China*

A new cosmological model based on the de Sitter gauge theory (dSGT) is studied in this paper. By some transformations, we find, in the dust universe, the cosmological equations of dSGT could form an autonomous system. We conduct dynamics analysis to this system, and find 9 critical points, among which there exist one positive attractor and one negative attractor. The positive attractor shows us that our universe will enter a exponential expansion phase in the end, which is similar to the conclusion of Λ CDM. We also carry out some numerical calculations, which confirms the conclusion of dynamics analysis. Finally, we fit the model parameter and initial values to the Union 2 SNIa dataset, present the confidence contour of parameters and obtain the best-fit values of parameters of dSGT.

I. INTRODUCTION

At the end of the last century, the astronomical observations of high redshift type Ia supernovae (SNIa) indicated that our universe is not only expanding, but also accelerating, which conflicts with our deepest intuition of gravity. With some other observations, such as cosmic microwave Background radiation (CMBR), baryon acoustic oscillations (BAO) and large-scale structure (LSS), physicists proposed a new standard cosmology model, Λ CDM, which introduces the cosmological constant back again. Although this unknown energy component accounts for 73% of the energy density of the universe, the measured value is too small to be explained by any current fundamental theories.[1]-[3] If one tries to solve this trouble phenomenologically by setting the cosmological constant to a particular value, the so-called fine-tuning problem would be brought up, which is considered as a basic problem almost any cosmological model would encounter. A good model should restrict the fine-tuning as much as possible. In order to alleviate this problem, various alternative theories have been proposed and developed these years, such as dynamical dark energy, modified gravity theories and even inhomogeneous universes. Recently, a new attempt, called torsion cosmology, has attracted researchers' attention, which introduces dynamical torsion to mimic the contribution of the cosmological constant. It seems more natural to use a pure geometric quantity to account for the cosmic acceleration than to introduce an exotic energy component.

Torsion cosmology could be traced back to the 1970s, and the early work mainly focused on issues of early universe, such as avoiding singularity and the origin of inflation. In some recent work, researchers attempted to extend the investigation to the current evolution and found it might account for the cosmic acceleration. Among these models, Poincaré gauge theory (PGT) cosmology is the one that has been investigated most widely. This model is based on PGT, which is inspired by the Einstein special relativity and the localization of global Poincaré symmetry[4]. Goenner *et al.* made a comprehensive survey of torsion cosmology and developed the equations for all the PGT cases.[5] Based on Goenner's work, Nester and his collaborators[6] found that the dynamical scalar torsion could be a possible reason for the accelerating expansion. Li *et al.*[7] extended the investigation to the late time evolution, which shows us the fate of our universe.

Besides PGT cosmology, there is another torsion cosmology, de Sitter gauge theory (dSGT) cosmology, which can also be a possible explanation to the accelerating expansion. This cosmological model is based on the de Sitter gauge theory, in which gravity is introduced as a gauge field from de Sitter invariant special relativity (dSSR), via the localization of de Sitter symmetry.[8] dSSR is a special relativity theory of the de Sitter space rather than the conventional Minkowski spacetime, which is another maximally symmetric spacetime with a uniform scalar curvature $1/R$. And the full symmetry group of this space is de Sitter group, which unifies the Lorentz group and the translation group, putting the spacetime symmetry in an alternatively interesting way. But in the limit of $R \rightarrow \infty$, the de Sitter group could also degenerate to the Poincaré group. To localize such a global symmetry, de Sitter symmetry, requires us to introduce certain gauge potentials which are found to represent the gravitational interaction. The gauge potential for de Sitter gauge theory is the de Sitter connection, which combines Lorentz connection and orthonormal tetrad, valued in $\mathfrak{so}(1,4)$ algebra. The gravitational action of dSGT takes the form of Yang-Mills gauge theory. Via variation of the

*Electronic address: aoxichen@gmail.com, kyhz@shnu.edu.cn

action with respect to the the Lorentz connection and orthonormal tetrad, one could attain the Einstein-like equations and gauge-like equations, respectively. These equations comprise a set of complicated non-linear equations, which are difficult to tackle. Nevertheless, if we apply them to the homogeneous and isotropic universe, these equations would be much more simpler and tractable. Based on these equations, one could construct an alternative cosmological model with torsion. Analogous to PGT, dSGT has also been applied to the cosmology recently to explain the accelerating expansion.[9]

Our main motivation of this paper is to investigate (i) whether the cosmological model based on de Sitter gauge theory could explain the cosmic acceleration; (ii) where we are going, i.e., what is the fate of our universe; (iii) the constraints of the parameters of model imposed by means of the comparison of observational data. By some analytical and numerical calculations, we found that, with a wide range of initial values, this model could account for the current status of the universe, an accelerating expanding, and the universe would enter an exponential expansion phase in the end.

This paper is organized as follows: First, we summarize the de Sitter gauge theory briefly in Sec. II, and then show the cosmological model based on de Sitter gauge theory in Sec. III. Second, we rewrite these dynamical equations as an autonomous system and do some dynamical analysis and numerical discussions on this system in the Sec. IV and V. Next in the VIth section, we compare the cosmological solutions to the SNIa data and constrain the parameters. Last of all, we discuss and summarize the implications of our findings in Section VII.

II. DE SITTER GAUGE THEORY OF GRAVITATION

In dSGT, the de Sitter connection is introduced as the gauge potential, which takes the form as

$$(\check{B}^{AB}_{\mu}) = \begin{pmatrix} B^{ab}_{\mu} & R^{-1}e^a_{\mu} \\ -R^{-1}e^b_{\mu} & 0 \end{pmatrix} \in \mathfrak{so}(1, 4), \quad (1)$$

where $\check{B}^{AB}_{\mu} = \eta^{BC}\check{B}^A_{C\mu}$, $\check{B}^{AB}_4 = \eta^{BC}\check{B}^A_{C4}$ and $\eta^{AB} = \text{diag}(1, -1, -1, -1, -1)$, which combines the Lorentz connection and the orthonormal tetrad¹. The associated field strength is the curvature of this connection, which is defined as

$$\check{F}_{\mu\nu} = (\check{F}^{AB}_{\mu\nu}) = \begin{pmatrix} F^{ab}_{\mu\nu} + R^{-2}e^{ab}_{\mu\nu} & R^{-1}T^a_{\mu\nu} \\ -R^{-1}T^b_{\mu\nu} & 0 \end{pmatrix} \in \mathfrak{so}(1, 4), \quad (2)$$

where $e^a_{b\mu\nu} = e^a_{\mu}e_{b\nu} - e^a_{\nu}e_{b\mu}$, $e_{a\mu} = \eta_{ab}e^b_{\mu}$, R is the de Sitter radius, and $F^{ab}_{\mu\nu}$ and $T^a_{\mu\nu}$ are the curvature and torsion of Lorentz-connection,

$$T^a_{\mu\nu} = \partial_{\mu}e^a_{\nu} - \partial_{\nu}e^a_{\mu} + B^a_{c\mu}e^c_{\nu} - B^a_{c\nu}e^c_{\mu}, \quad (3)$$

$$F^a_{b\mu\nu} = \partial_{\mu}B^a_{b\nu} - \partial_{\nu}B^a_{b\mu} + B^a_{c\mu}B^c_{b\nu} - B^a_{c\nu}B^c_{b\mu}, \quad (4)$$

which also satisfy the respective Bianchi identities.

The gauge-like action of gravitational fields in dSGT takes the form, [9]

$$S_G = \frac{\hbar}{4g^2} \int_{\mathcal{M}} d^4x e \mathbf{Tr}_{dS}(\check{F}_{\mu\nu}\check{F}^{\mu\nu}) \quad (5)$$

$$= - \int_{\mathcal{M}} d^4x e \left[\frac{\hbar}{4g^2} F^{ab}_{\mu\nu} F^{ab\mu\nu} - \chi \left(F - \frac{6}{R^2} \right) - \frac{\chi}{2} T^a_{\mu\nu} T^a{}^{\mu\nu} \right]. \quad (6)$$

Here, $e = \det(e^a_{\mu})$, g is a dimensionless constant describing the self-interaction of the gauge field, χ is a dimensional coupling constant related to g and R , and $F = -\frac{1}{2}F^{ab}_{\mu\nu}e^{a\mu}e^{b\nu}$ is the scalar curvature of the Cartan connection. In order to be consistent with Einstein-Cartan theory, we take $\chi = 1/(16\pi G)$ and $\hbar g^{-2} = 3\chi\Lambda^{-1}$, where $\Lambda = 3/R^2$.

Assuming that the matter is minimally coupled to gravitational fields, the total action of dSGT could be written as:

$$S_T = S_G + S_M, \quad (7)$$

¹ In this paper, the Greek indices, μ, ν, \dots , are 4D coordinate indices, whereas the capital Latin indices A, B, C, \dots , and the lowercase Latin indices, a, b, \dots , denote 5D and 4D orthonormal tetrad indices, respectively.

where S_M denotes the action of matter, namely the gravitational source. Now we can obtain the field equations via variational principle with respect to e_μ^a, B_{μ}^{ab} ,

$$\begin{aligned} \nabla_\nu T_a^{\mu\nu} - F_a^\mu + \frac{1}{2} F e_a^\mu - \Lambda e_a^\mu - \frac{8\pi G\hbar}{g^2} \left(e_a^\kappa \text{Tr}(F^{\mu\lambda} F_{\kappa\lambda}) - \frac{1}{4} e_a^\mu \text{Tr}(F^{\lambda\sigma} F_{\lambda\sigma}) \right) \\ - 16\pi G\chi \left(e_a^\kappa T_b^{\mu\lambda} T_{\kappa\lambda}^b - \frac{1}{4} e_a^\mu T_b^{\lambda\sigma} T_{\lambda\sigma}^b \right) = 8\pi G T_{Ma}^\mu \end{aligned} \quad (8)$$

$$\nabla_\nu F_{ab}^{\mu\nu} - R^{-2} \left(Y_{\lambda\nu}^\mu e_{ab}^{\lambda\nu} + Y_{\lambda\nu}^\nu e_{ab}^{\mu\lambda} + 2T_{[a}^{\mu\lambda} e_{b]\lambda} \right) = 16\pi G R^{-2} S_{Mab}^\mu, \quad (9)$$

where

$$T_{Ma}^\mu := -\frac{1}{e} \frac{\delta S_M}{\delta e_\mu^a}, \quad S_{Mab}^\mu := \frac{1}{2\sqrt{-g}} \frac{\delta S_M}{\delta B_{\mu}^{ab}}, \quad (10)$$

represent the effective energy-momentum density and spin density of the source, respectively, and

$$Y_{\lambda\nu}^\nu := \frac{1}{2} (T_{\nu\mu}^\lambda + T_{\mu\nu}^\lambda + T_{\nu}^{\lambda\mu}), \quad (11)$$

is the contorsion. It is worth noticing that the Nabla operator in Eq. (8) and (9) is the covariant derivative compatible with Christoffel symbols $\{\mu_{\nu\kappa}\}$ for coordinate indices, and Lorentz connection $B_{b\mu}^a$ for orthonormal tetrad indices. Readers can be referred to Ref.[9] for more details on dSGT.

III. THE COSMOLOGICAL EVOLUTION EQUATIONS

Since current observations favor a homogeneous, isotropic universe, we here work on a Robertson-Walker (RW) cosmological metric

$$ds^2 = dt^2 - a(t)^2 \left[\frac{dr^2}{1 - kr^2} + r^2(d\theta^2 + \sin^2\theta d\phi^2) \right]. \quad (12)$$

For Robertson-Walker metric, the nonvanishing torsion tensor components are of the form ²,

$$T_{j0}^i(t) = T_+(t) \delta_j^i, \quad T_{jk}^i(t) = T_-(t) \epsilon^i_{jk}, \quad (13)$$

where T_+ denotes the vector piece of torsion, namely, in components, the trace of the torsion, and T_- indicates the axial-vector piece of torsion, which corresponds in components to the totally antisymmetric part of torsion. T_+ and T_- are both functions of time t , and their subscripts, $+$ and $-$, denote the even and odd parities, respectively.

The nonvanishing torsion 2-forms in this case are

$$\begin{aligned} \mathbf{T}^0 &= 0 \\ \mathbf{T}^1 &= T_+ \vartheta^0 \wedge \vartheta^1 + T_- \vartheta^2 \wedge \vartheta^3 \\ \mathbf{T}^2 &= T_+ \vartheta^0 \wedge \vartheta^2 + T_- \vartheta^3 \wedge \vartheta^1 \\ \mathbf{T}^3 &= T_+ \vartheta^0 \wedge \vartheta^3 + T_- \vartheta^1 \wedge \vartheta^2, \end{aligned} \quad (14)$$

where $\vartheta^0 = dt$, $\vartheta^1 = \frac{a(t)dr}{\sqrt{1-kr^2}}$, $\vartheta^2 = a(t)r d\theta$ and $\vartheta^3 = a(t)r \sin\theta d\phi$.

² Here, the Latin indices i, j, k, \dots , are 3D orthonormal tetrad indices with range 1, 2, 3.

According to the RW metric Eq.(12) and the torsion Eq. (13), the field equations could be reduced to

$$\begin{aligned} & -\frac{\ddot{a}^2}{a^2} - \left(\dot{T}_+ + 2\frac{\dot{a}}{a}T_+ - 2\frac{\ddot{a}}{a} \right) \dot{T}_+ + \frac{1}{4} \left(\dot{T}_- + 2\frac{\dot{a}}{a}T_- \right) \dot{T}_- + T_+^4 - \frac{3}{2}T_+^2T_-^2 + \frac{1}{16}T_-^4 + \left(5\frac{\dot{a}^2}{a^2} \right. \\ & \quad \left. + 2\frac{k}{a^2} - \frac{3}{R^2} \right) T_+^2 - \frac{1}{2} \left(\frac{5}{2}\frac{\dot{a}^2}{a^2} + \frac{k}{a^2} - \frac{3}{R^2} \right) T_-^2 + 2\frac{\dot{a}}{a} \left(\frac{\ddot{a}}{a} - 2\frac{\dot{a}^2}{a^2} - 2\frac{k}{a^2} + \frac{3}{R^2} \right) T_+ - \frac{\dot{a}}{a}(4T_+^2 \\ & \quad - 3T_-^2)T_+ + \frac{\dot{a}^2}{a^2} \left(\frac{\dot{a}^2}{a^2} + 2\frac{k}{a^2} - \frac{2}{R^2} \right) + \frac{k^2}{a^4} - \frac{2}{R^2}\frac{k}{a^2} + \frac{2}{R^4} = -\frac{16\pi G\rho}{3R^2}, \end{aligned} \quad (15)$$

$$\begin{aligned} & \frac{\ddot{a}^2}{a^2} + \left(\dot{T}_+ + 2\frac{\dot{a}}{a}T_+ - 2\frac{\ddot{a}}{a} + \frac{6}{R^2} \right) \dot{T}_+ - \frac{1}{4} \left(\dot{T}_- + 2\frac{\dot{a}}{a}T_- \right) \dot{T}_- - T_+^4 + \frac{3}{2}T_+^2T_-^2 - \frac{1}{16}T_-^4 \\ & \quad + \frac{\dot{a}}{a}(4T_+^2 - 3T_-^2)T_+ - \left(5\frac{\dot{a}^2}{a^2} + 2\frac{k}{a^2} + \frac{3}{R^2} \right) T_+^2 + \frac{1}{2} \left(\frac{5}{2}\frac{\dot{a}^2}{a^2} + \frac{k}{a^2} + \frac{3}{R^2} \right) T_-^2 - 2\frac{\dot{a}}{a} \left(\frac{\ddot{a}}{a} - 2\frac{\dot{a}^2}{a^2} \right. \\ & \quad \left. - 2\frac{k}{a^2} - \frac{6}{R^2} \right) T_+ - \frac{4}{R^2}\frac{\ddot{a}}{a} - \frac{\dot{a}^2}{a^2} \left(\frac{\dot{a}^2}{a^2} + 2\frac{k}{a^2} \right) + \frac{2}{R^2} - \frac{k^2}{a^4} - \frac{2}{R^2}\frac{k}{a^2} + \frac{6}{R^4} = -\frac{16\pi Gp}{R^2}, \end{aligned} \quad (16)$$

$$\ddot{T}_- + 3\frac{\dot{a}}{a}\dot{T}_- + \left(\frac{1}{2}T_-^2 - 6T_+^2 + 12\frac{\dot{a}}{a}T_+ + \frac{\ddot{a}}{a} - 5\frac{\dot{a}^2}{a^2} - 2\frac{k}{a^2} + \frac{6}{R^2} \right) T_- = 0, \quad (17)$$

$$\begin{aligned} & \ddot{T}_+ + 3\frac{\dot{a}}{a}\dot{T}_+ - \left(2T_+^2 - \frac{3}{2}T_-^2 - 6\frac{\dot{a}}{a}T_+ - \frac{\ddot{a}}{a} + 5\frac{\dot{a}^2}{a^2} + 2\frac{k}{a^2} - \frac{3}{R^2} \right) T_+ - \frac{3}{2}\frac{\dot{a}}{a}T_-^2 - \frac{\ddot{a}}{a} - \frac{\dot{a}\ddot{a}}{a^2} \\ & \quad + 2\frac{\dot{a}^3}{a^3} + 2\frac{\dot{a}}{a}\frac{k}{a^2} = 0, \end{aligned} \quad (18)$$

where Eqs.(15) and (16) are the (t, t) and (r, r) component of Einstein-like equations, respectively; and Eqs.(17) and (18) are 2 independent Yang-like equations, which is derived from the (r, θ, ϕ) and (t, r, r) components of Lorentz connection. The spin density of present time is generally thought be very small which could be neglected. Therefore, we here assumed the spin density is zero.

The Bianchi identities ensure that the energy momentum tensor is conserved, which leads to the continuity equation:

$$\dot{\rho} = -\frac{3\dot{a}}{a}(\rho + p). \quad (19)$$

Equation (19) can also be derived from Eqs. (15)- (18), which means only four of Eqs. (15)- (19) are independent. With the equation of state (EoS) of matter content, these four equations comprise a complete system of equations for five variables, $a(t), T_+(t), T_-(t), \rho(t)$ and $p(t)$. By some algebra and differential calculations, we could simplify these 5 equations as:

$$\begin{aligned} \dot{H} &= -2H^2 - \frac{k}{a^2} + \frac{2}{R^2} + \frac{4\pi G}{3}(\rho + 3p) + \frac{3}{2} \left(\dot{T}_+ + 3HT_+ - T_+^2 + \frac{T_-^2}{2} \right) \\ & \quad + (1 + 3w)\rho, \end{aligned} \quad (20)$$

$$\begin{aligned} \ddot{T}_+ &= -3 \left(H + \frac{3}{2}T_+ \right) \dot{T}_+ - 3T_- \dot{T}_- - \frac{8\pi G}{3}(\rho + 3p) - \frac{3}{2}HT_-^2 + \left[\frac{13}{2}(T_+ - 3H)T_+ \right. \\ & \quad \left. + 6H^2 + \frac{3k}{a^2} + \frac{9T_-^2}{4} - \frac{8}{R^2} - \frac{28\pi G}{3}(\rho + 3p) \right] T_+, \end{aligned} \quad (21)$$

$$\begin{aligned} \ddot{T}_- &= -3H\dot{T}_- - \left[-\frac{15}{2}T_+^2 + \frac{33HT_+}{2} - 6H^2 - \frac{3k}{a^2} + \frac{8}{R^2} + \frac{5}{4}T_-^2 + \frac{3}{2}\dot{T}_+ \right. \\ & \quad \left. + \frac{4\pi G}{3}(\rho + 3p) \right] T_-, \end{aligned} \quad (22)$$

$$\dot{\rho} = -3H(\rho + p), \quad (23)$$

$$w = \frac{p}{\rho}, \quad (24)$$

where $H = \dot{a}/a$ is the Hubble parameter.

	Critical Points	Eigenvalues
(i)	$(\frac{1}{R}, 0, 0, 0, 0, 0)$	$-\frac{1}{R}, -\frac{1}{R}, -\frac{2}{R}, -\frac{2}{R}, -\frac{3}{R}, -\frac{4}{R}$
(ii)	$(-\frac{1}{R}, 0, 0, 0, 0, 0)$	$\frac{1}{R}, \frac{1}{R}, \frac{2}{R}, \frac{2}{R}, \frac{3}{R}, \frac{4}{R}$
(iii)	$(-\frac{1}{2R}, 0, 0, -\frac{2}{R}, 0, 0)$	$-\frac{2}{R}, \frac{2}{R}, \frac{3}{2R}, -\frac{5}{2R}, \frac{7}{2R}, \frac{4}{R}$
(iv)	$(\frac{1}{2R}, 0, 0, \frac{2}{R}, 0, 0)$	$-\frac{2}{R}, \frac{2}{R}, \frac{5}{2R}, -\frac{3}{2R}, -\frac{4}{R}, -\frac{7}{2R}$
(v)	$(-\frac{1}{2R}, 0, 0, \frac{1}{2R}, 0, 0)$	$\frac{1}{2R}, \frac{1}{R}, -\frac{1}{R}, \frac{2}{R}, \frac{3}{2R}, \frac{5}{2R}$
(vi)	$(\frac{1}{2R}, 0, 0, -\frac{1}{2R}, 0, 0)$	$-\frac{1}{2R}, \frac{1}{R}, -\frac{1}{R}, -\frac{3}{2R}, -\frac{5}{2R}, -\frac{2}{R}$
(vii)	$(0, 0, 0, -\frac{\sqrt{3/2}}{R}, 0, \frac{1}{4R^2})$	$-\frac{\sqrt{3}}{\sqrt{2R}}, \frac{\sqrt{3}}{\sqrt{2R}}, -\frac{\sqrt{3}}{R}, \frac{\sqrt{3}}{R}, -\frac{\sqrt{6}}{R}, \frac{\sqrt{6}}{R}$
(viii)	$(0, 0, 0, \frac{\sqrt{3/2}}{R}, 0, \frac{1}{4R^2})$	$-\frac{\sqrt{3}}{\sqrt{2R}}, \frac{\sqrt{3}}{\sqrt{2R}}, -\frac{\sqrt{3}}{R}, \frac{\sqrt{3}}{R}, -\frac{\sqrt{6}}{R}, \frac{\sqrt{6}}{R}$
(ix)	$(0, 0, 0, 0, 0, \frac{-2}{R^2})$	$-\frac{\sqrt{3}-3i}{\sqrt{2R}}, \frac{\sqrt{3}-3i}{\sqrt{2R}}, -\frac{\sqrt{3}+3i}{\sqrt{2R}}, \frac{\sqrt{3}+3i}{\sqrt{2R}}, -\frac{i\sqrt{6}}{R}, \frac{i\sqrt{6}}{R}$

TABLE I: The critical points and their corresponding eigenvalues. The point 9 is not physically acceptable, for its negative energy density.

IV. AUTONOMOUS SYSTEM

If we rescale the variables and parameters as

$$\begin{aligned}
t &\rightarrow t/l_0; & H &\rightarrow l_0 H; & k &\rightarrow l_0^2 k; & R &\rightarrow R/l_0; \\
T_{\pm} &\rightarrow l_0 T_{\pm}; & \rho &\rightarrow \frac{4\pi G l_0^2}{3} \rho; & p &\rightarrow \frac{4\pi G l_0^2}{3} p,
\end{aligned} \tag{25}$$

where $l_0 = 1/H_0$ is the Hubble radius in natural units, these variables and parameters would be dimensionless. Under this transformation, Eqs. (20)-(24) remain unchanged expect for the terms including $4\pi G\rho/3$ and $4\pi Gp/3$, which change into ρ and p respectively. The contribution of radiation and spatial curvature in current universe are so small that it could be neglected, so we here just consider the dust universe with spatial flatness, whose EoS is equal to zero. By some further calculations, these equations could be transformed to a set of six one-order ordinary derivative equations, which forms a six-dimensional autonomous system, as follows,

$$\dot{H} = -2H^2 + \frac{2}{R^2} + \frac{3}{2} \left(P + 3HT_+ - T_+^2 + \frac{T_-^2}{2} \right) + \rho, \tag{26}$$

$$\begin{aligned}
\dot{P} = & -3 \left(H + \frac{3}{2}T_+ \right) P - 3T_-Q - \frac{3}{2}HT_-^2 + \left[\frac{13}{2}(T_+ - 3H)T_+ + 6H^2 \right. \\
& \left. + \frac{9T_-^2}{4} - \frac{8}{R^2} - 7\rho \right] T_+ + 6H\rho,
\end{aligned} \tag{27}$$

$$\dot{T}_+ = P, \tag{28}$$

$$\dot{Q} = -3HQ - \left(-\frac{15}{2}T_+^2 + \frac{33HT_+}{2} - 6H^2 + \frac{8}{R^2} + \frac{5}{4}T_-^2 + \frac{3}{2}P + \rho \right) T_-, \tag{29}$$

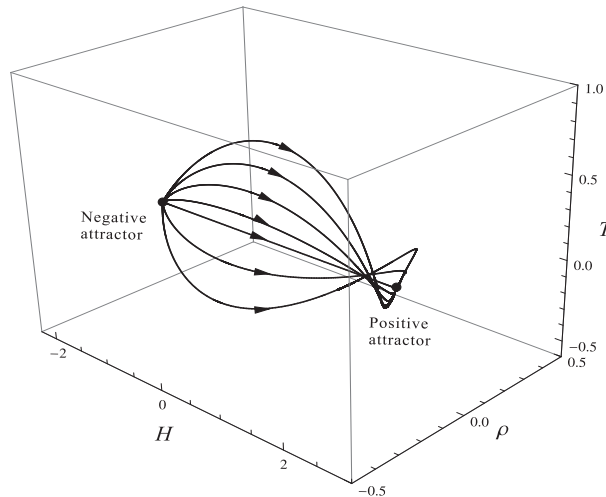
$$\dot{T}_- = Q, \tag{30}$$

$$\dot{\rho} = -3H\rho. \tag{31}$$

For such an autonomous system, we can use the dynamics analysis to investigate its qualitative properties. Critical points are some exact constant solutions in the autonomous system, which indicate the asymptotic behavior of evolution. For example, some solutions, such as heteroclinic orbits, connect two different critical points, and some others, such as homoclinic orbits, are a closed loop starting from and coming back to the same critical point. In the dynamics analysis of cosmology, the heteroclinic orbit is more interesting.[10] Thus, critical points could be treated as the basic tool in dynamics analysis, from which one could know the qualitative properties of the autonomous system. By some algebra calculation, we find all the 9 critical points (H_c , P_c , Q_c , T_{+c} , T_{-c} , ρ_c) of this system, as shown in Table 1. Furthermore, we analyze the stabilities of these critical points by means of the first-order perturbations. Substituting these linear perturbations into these dynamical equations, we would obtain the perturbation equations

Critical Points	Property	Stability
(i)	Positive-Attractor	Stable
(ii)	Negative-Attractor	Unstable
(iii)	Saddle	Unstable
(iv)	Saddle	Unstable
(v)	Saddle	Unstable
(vi)	Saddle	Unstable
(vii)	Saddle	Unstable
(viii)	Saddle	Unstable
(ix)	Spiral-Saddle	Unstable

TABLE II: The stability properties of critical points

FIG. 1: The (H, T_+, ρ) section of the phase diagram with $R=4/3$. The heteroclinic orbits connect the critical point (i) and (ii).

around the critical points, i.e.

$$\delta \dot{\mathbf{x}} = A \mathbf{x}, \quad A = \left. \frac{\partial \mathbf{f}}{\partial \mathbf{x}} \right|_{\mathbf{x}=\mathbf{x}_c}, \quad (32)$$

where x means the six variables of this autonomous system and f denotes the corresponding vector function on the right-hand side of Eqs. (26)-(31). Using the coefficient matrix A 's eigenvalue, we could analyze the stabilities of these critical points. And the classification of these critical points is shown in Table II. Among these critical points, there are only one positive attractor, i.e. point (i), whose eigenvalues are all negative, and only one negative attractor, i.e. point (ii), whose eigenvalues are all positive. The negative attractor works as a source, from which the phase orbits start off, whereas the positive attractor works as a sink, which the orbits finally approach. And it is the heteroclinic line that connects the positive attractor and the negative attractor, as shown in Fig. 1. Positive attractors are stable exact solutions, describing the infinite future behavior of evolution, while the unstable negative attractors depict the stories of infinite past. Therefore the positive attractor, point (i), here shows us the picture of late time universe, where all quantities tend to zero, except the Hubble parameter which approaches a finite value. At that time, the whole universe is entering an exponential expansion phase, just like the Λ CDM model.

V. NUMERICAL DEMONSTRATION

In order to confirm these qualitative results derived from dynamics analysis and know better about the global properties of this model, we explore the autonomous system by numerical methods. To solve the Eqs. (26)-(31) numerically, we choose some generic initial conditions and parameters, as shown in Table III. First, we vary initial conditions $(P_0, Q_0, T_{-0}, T_{+0}, \rho_0)$ with a fixed de Sitter radius, and the results are shown in Fig.2(a). Then we change the de Sitter radius, and show the results in Fig.2(b). Because of the rescaling Eqs. (25), the current Hubble parameter

Case	R	H_0	P_0	Q_0	T_{+0}	T_{-0}	ρ_0
(a.1)	1.5	1	0	0	0	0	0.5
(a.2)	1.5	1	0	-0.5	-0.5	0	1
(a.3)	1.5	1	-0.75	-1	2	1.2	0.7
(b.1)	0.4	1	0	0	-1.5	0	0.8
(b.2)	0.6	1	0	0	-1	0	1
(b.3)	1.5	1	0	0	0	0	0.5

TABLE III: The values of initial conditions and parameters for the evolution curves in Fig. 2.

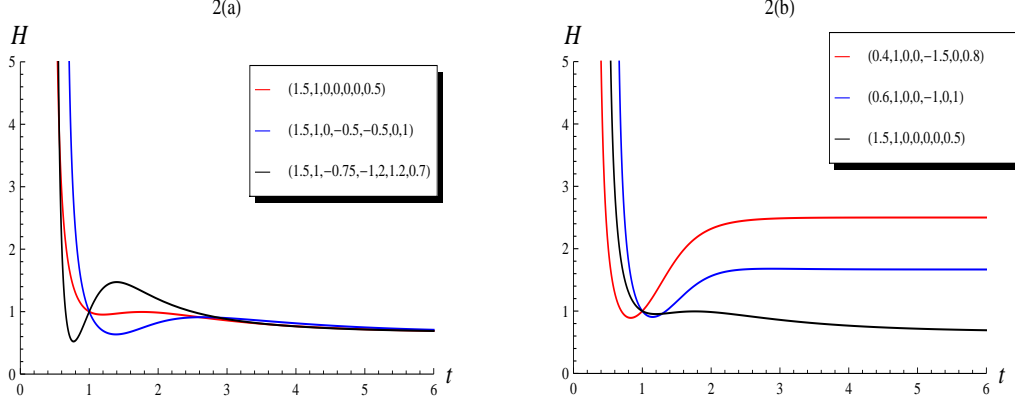


FIG. 2: The evolution of Hubble parameter H with respect to some initial values and parameter choice $(R, H_0, P_0, Q_0, T_{+0}, T_{-0}, \rho_0)$. According to the transformations (25), the unit of time here is the Hubble Time. In Fig 2(a), we fixed R and changed T_{\pm} , while in Fig 2(b), we changed R .

here must be 1. From these numerical results, it is easy to find that the Hubble parameter of all the solutions approaches a particular finite value in the infinite future, whatever the initial conditions are, and this value only depends on the de Sitter radius R . Such results demonstrate the dynamics analysis we have done in the former section. We could also find that this positive attractor covers a wide range of initial conditions, and therefore the troublesome fine-tuning problem has been alleviated. In comparison with the result of PGT, we find the cosmology based on de Sitter gauge theory is quite different from the Poincare gauge theory, where the expansion will asymptotically come to a halt. It is the existence of the de Sitter radius that makes such a discrepancy. If we let $R \rightarrow \infty$, the de Sitter gauge theory would degenerate to the PGT.

VI. SUPERNOVAE DATA FITTING

A basic approach to testing a cosmological model is the supernova fitting through its description of the expansion history of the universe. In this section we fit the initial conditions and model parameters to current type Ia supernovae data. And the maximum likelihood technique is used here, which could determine the best fit values of parameters and initial conditions and the goodness of this model. The supernova data are comprised of the distance modulus μ_{obs} , which is equal to the difference between apparent magnitude m_i and absolute magnitude M_i , and redshifts z_i of supernovae with their corresponding errors σ_i . Note that the error here are assumed to be normally distributed and independent.

The theoretical distance modulus is related to the luminosity distance d_L by

$$\begin{aligned}
 \mu_{th}(z_i) &= 5 \log_{10} \left(\frac{d_L(z_i)}{\text{Mpc}} \right) + 25 \\
 &= 5 \log_{10} D_L(z_i) - 5 \log_{10} \left(\frac{cH_0^{-1}}{\text{Mpc}} \right) + 25 \\
 &= 5 \log_{10} D_L(z_i) - 5 \log_{10} h + 42.38,
 \end{aligned} \tag{33}$$

where the $D_L(z)$ is the dimensionless 'Hubble-constant free' luminosity defined by $D_L(z) = H_0 d_L(z)/c$.

For a spatially flat cosmological model, which we consider here, the luminosity distance could be expressed in terms of Hubble parameter $H(z)$, as follows,

$$D_L(z) = (1+z) \int_0^z dz' \frac{1}{H(z'; a_1, \dots, a_n)}, \quad (34)$$

where the Hubble parameter $H(z'; a_1, \dots, a_n)$ here is the dimensionless Hubble parameter under the rescaling transformation Eq (25).

As we know, due to the normal distribution of errors, we could use the χ^2 parameter as the maximum likelihood estimator to determine the best fit values of parameters and initial conditions ($R, P_0, Q_0, T_{+0}, T_{-0}, \rho_0$) of the model. The χ^2 here for the SNIa data is

$$\begin{aligned} \chi^2(\theta) &= \sum_i^N \frac{[\mu_{obs}(z_i) - \mu_{th}(z_i)]^2}{\sigma_i^2}, \\ &= \sum_i^N \frac{[\mu_{obs}(z_i) - 5 \log_{10} D_L(z_i; \theta) - \mu_0]^2}{\sigma_i^2}, \end{aligned} \quad (35)$$

where $\mu_0 = -5 \log_{10} h + 42.38$, θ denotes all the parameters and initial conditions, and σ_i are the statistical errors of SNIa. If we want to include the systematic errors, which are comparable to the statistical errors and should be taken into account seriously, we could resort to the covariance matrix C_{SN} , and the Eq. (35) turn out to take the form

$$\chi^2(\theta) = \sum_{i,j}^N [\mu_{obs}(z_i) - \mu_{th}(z_i)] (C_{SN}^{-1})_{ij} [\mu_{obs}(z_j) - \mu_{th}(z_j)], \quad (36)$$

$$= \sum_{i,j}^N [\mu_{obs}(z_i) - 5 \log_{10} D_L(z_i; \theta) - \mu_0] (C_{SN}^{-1})_{ij} [\mu_{obs}(z_j) - 5 \log_{10} D_L(z_j; \theta) - \mu_0]. \quad (37)$$

The parameter μ_0 here is a nuisance parameter, whose contribution we are not interested in. So we marginalize over this parameter, μ_0 , thus obtaining a new χ^2 ,

$$\chi^2(\theta) = A(\theta) - \frac{B(\theta)^2}{C} + \ln \left(\frac{C}{2\pi} \right), \quad (38)$$

where

$$A(\theta) = \sum_{i,j}^N [\mu_{obs}(z_i; \theta) - 5 \log_{10} D_L(z_i; \theta)] (C_{SN}^{-1})_{ij} [\mu_{obs}(z_j; \theta) - 5 \log_{10} D_L(z_j; \theta)], \quad (39)$$

$$B(\theta) = \sum_j^N (C_{SN}^{-1})_{ij} [\mu_{obs}(z_j; \theta) - 5 \log_{10} D_L(z_j; \theta)], \quad (40)$$

$$C(\theta) = \sum_{i,j}^N = (C_{SN}^{-1})_{ij}. \quad (41)$$

Now we try to constrain our model parameter and initial values by this maximum likelihood estimator. The dataset we use here is the “Union2” SNIa dataset (N=557), the most comprehensive one to date, which combines all the previous SNIa dataset in a homogeneous manner.

By minimizing the χ^2 , we find the best fit parameters of dSGT model, as shown in Table. IV Based on the current

Case	R	P_0	Q_0	T_{+0}	T_{-0}	ρ_0	χ^2
I.	1.1005	0	0	0	0	0.0431	535.3384

TABLE IV: The best-fit initial data and parameters

observations, the present density of torsion in our universe is very small, so it is reasonable to assume that the initial values of all torsions and their first order derivative are zero at $z = 0$. But their second order derivatives does not

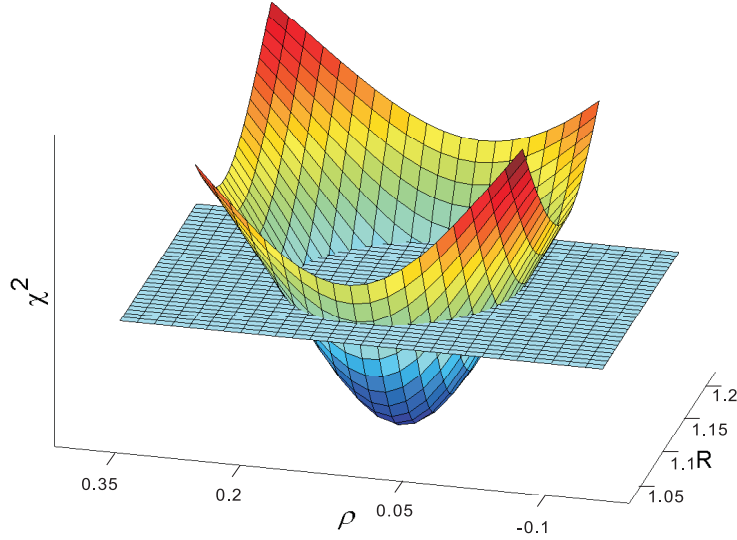


FIG. 3: The χ^2 distribution with respect to R and ρ , compared to the Λ CDM, the plane $\chi^2 = 536.634$. Here we assume that all the torsions and their first order derivatives vanish at present time.

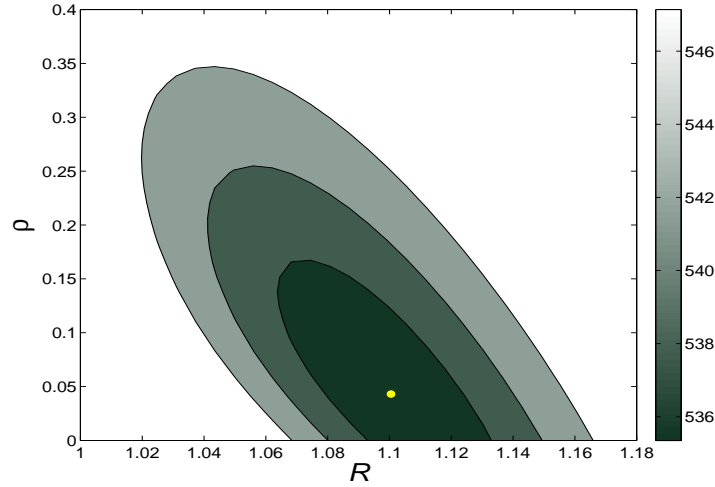


FIG. 4: The 68.3%, 95.4% and 99.7% χ^2 confidence contours of dSGT with respect to R and ρ , using the Union 2 dataset. Here we also assume that the current-time values for all the torsions and their first order derivatives are zero. The yellow point is the best-fit point.

vanish yet, which would have a significant impact on the history and future of the evolution of our universe. In this case, the number of parameter and initial value is reduced, and the rest parameters and initial values are just R and ρ_0 . It is easy to find the best-fit of these 2 parameters, which are shown in Table IV. And the minimal χ^2 is 535.3384, whereas the value for Λ CDM is 536.634, with $\Omega_m = 0.27, \Omega_\Lambda = 0.73$. In Fig. 3 we show the χ^2 distribution with respect to R and ρ compared to Λ CDM model, where the plane $\chi^2 = 536.635$ corresponds to the value of Λ CDM. Furthermore, we plot the contours of some particular confidence levels, as shown in Fig. 4. From these figures, we could find that the evolution of our universe is insensitive to the initial value, which alleviate the fine-tuning problem.

VII. SUMMARY AND CONCLUSION

The astronomical observations imply that our universe is accelerating to a de Sitter spacetime. This gives us a strong motive to consider the cosmic evolution based on the de Sitter gauge theory instead of other gravity theories. The localization of de Sitter symmetry requires us to introduce curvature and torsion. So in de Sitter gauge theory, the torsion is an indispensable quantity, by which people tried to include the effect of spin density in gravity theory at first. But now this essential quantity might account for the acceleration of our universe, if we apply dSGT to cosmology.

We found the cosmological equations for dust universe in dSGT could form an autonomous system by some transformations, where the evolution of the universe is described in terms of the orbits in phase space. Therefore, by dynamics analysis to the dSGT cosmology, one could study the qualitative properties of this phase space. We found all 9 critical points, as shown in Table I. We also analyzed the stabilities of these critical points, and found among these critical points there is only one positive attractor, which is stable. The positive attractor alleviates the fine-tuning problem and implies that the universe will expand exponentially in the end, whereas all other physical quantities will turn out to vanish. In this sense, dSGT cosmology looks more like the Λ CDM, than PGT cosmology. And we conducted some concrete numerical calculations of this the destiny of our model of the universe, which confirms conclusions from dynamics analysis.

Finally, in order to find the best-fit values and constraints of model parameters and initial conditions, we fitted them to the Union 2 SNIa dataset. The maximum likelihood estimator here we used is the χ^2 estimate. By minimizing the χ^2 , we found the best-fit parameters $R = 1.135$, $\rho = 0.274$ and the corresponding $\chi^2 = 535.3384$, while the value for Λ CDM is 536.634, with $\Omega_m = 0.27$, $\Omega_\Lambda = 0.73$. Note that we here set all the initial values of torsions and their first-order derivatives to zero at $t = t_0$, since the contribution of torsion to the current universe is almost negligible. We also plotted the confidence contour Fig. 4 with respect to R and ρ , from which it is easy to see that the fine-tuning problem is alleviated and the evolution is not so sensitive to the initial values and model parameters.

If we want to go deeper into cosmology based on de Sitter gauge theory, there are a lot of work need to be done. We should fit this model to some other observations, like BAO and LSS etc, to constrain the parameters better. We also could study the perturbations in the early universe, and compare the results to CMBR data. These issues will considered in some upcoming papers.

Acknowledgments

This work is supported by SRFDP under Grant No. 200931271104 and Shanghai Natural Science Foundation, China, under Grant No. 10ZR1422000.

-
- [1] P. J. E. Peebles and B. Ratra, *The cosmological constant and dark energy*, *Rev. Mod. Phys.* **75** (2003) 559-606, [astro-ph/0207347].
 - [2] T. Padmanabhan, *Cosmological constant: The weight of the vacuum*, *Phys. Rept.* **380** (2003) 235-320, [hep-th/0212290]; X.-Z. Li and J.-G. Hao, *O(N) phantom, a way to implement $w < -1$* *Phys. Rev.* **D69** (2004) 107303, [hep-th/0303093].
 - [3] J.-G. Hao and X.-Z. Li, *Phantom Cosmic Dynamics: Tracking Attractor and Cosmic Doomsday*, *Phys. Rev.* **D70** (2004) 043529, [astro-th/0309746]; C.-J. Feng and X.-Z. Li, *Cardassian Universe Constrained by Latest Observations* *Phys. Lett.* **B692** (2010) 152-156, [arXiv:0912.4793].
 - [4] F. W. Hehl, *Four lectures on Poincaré gauge field theory* in *Proc. of the 6th Course of the School of Cosmology and Gravitation on Spin, Torsion, Rotation, and Supergravity*, eds. P. G. Bergmann and V. De Sabbata (New York: Plenum) p5
M. Blagojević, *Gravitation and Gauge Symmetries*, IoP Publishing, Bristol, 2002.
 - [5] H. Goenner and F. Müller-Hoissen *Spatially homogeneous and isotropic spaces in theories of gravitation with torsion*, *Class. Quantum Grav.* **1** (1984) 651-672.
 - [6] H. Chen, F.-H. Ho and J. M. Nester, C.-H. Wang, and H.-J. Yo, *Cosmological dynamics with propagating Lorentz connection modes of spin zero*, *JCAP* **0910** (2009) 027, [arXiv:0908.3323];
P. Baekler, F. W. Hehl, and J. M. Nester, *Poincaré gauge theory of gravity: Friedman cosmology with even and odd parity modes. Analytic part*, *Phys. Rev.* **D83** (2011) 024001, [arXiv:1009.5112];
F.-H. Ho and J. M. Nester, *Poincaré Gauge Theory With Coupled Even And Odd Parity Dynamic Spin-0 Modes: Dynamic Equations For Isotropic Bianchi Cosmologies*, [arXiv:1106.0711];
F.-H. Ho and J. M. Nester, *Poincaré gauge theory with even and odd parity dynamic connection modes: isotropic Bianchi cosmological models*, [arXiv:1105.5001].

- [7] X.-Z. Li, C.-B. Sun, and P. Xi, *Torsion cosmological dynamics*, *Phys. Rev.* **D79** (2009) 027301, [arXiv:0903.3088];
X.-Z. Li, C.-B. Sun, and P. Xi, *Statefinder diagnostic in a torsion cosmology*, *JCAP* **0904** (2009) 015, [arXiv:0903.4724];
X.-C. Ao, X.-Z. Li, and P. Xi *Analytical approach of late-time evolution in a torsion cosmology* *Phys. Lett.* **B694** (2010) 186-190, [arXiv:101.4117].
- [8] H.-Y. Guo, C.-G. Huang, Z. Xu, and B. Zhou, *On Beltrami model of de Sitter spacetime*, *Mod. Phys. Lett.* **A19** (2004) 1701-1710, [hep-th/0311156];
H.-Y. Guo, C.-G. Huang, Z. Xu, and B. Zhou, *On special relativity with cosmological constant*, *Phys. Lett.* **A331** (2004) 1-7, [hep-th/043171];
H.-Y. Guo, C.-G. Huang, Z. Xu, and B. Zhou, *Three kinds of special relativity via inverse Wick rotation*, *Chin. Phys. Lett.* **22** (2005) 2477-2480, [hep-th/0508094];
H.-Y. Guo, C.-G. Huang, B. Zhou, *Temperature at horizon in de Sitter spacetime*, *Europhys. Lett.* **72** (2005) 1045-1051.
- [9] C.-G. Huang, H.-Q. Zhang, and H.-Y. Guo, *Cosmological Solutions with Torsion in a Model of de Sitter Gauge Theory of Gravity* *JCAP* **0810** (2008) 010, [arXiv:0801.0905].
- [10] X.-Z. Li, Y.-B. Zhao, and C.-B. Sun, *Heteroclinic orbit and tracking attractor in cosmological model with a double exponential potential*, *Class. Quant. Grav.* **22** (2005) 3759-3766, [astro-ph/050819];
J.-G. Hao and X.-Z. Li, *An attractor solution of phantom field*, *Phys. Rev.* **D67** (2003) 107303, [gr-qc/0302100].